Journal of Civil Engineering and Architecture 9 (2015) 1439-1451
doi: 10.17265/1934-7359/2015.12.006

Tensile Characteristics Evaluation of Corroded Reinforcing Bars Extracted from Actual Structures

Toshiyuki Kanakubo[1] and Michiaki Oyado[2]

1. Division of Engineering Mechanics and Energy, Faculty of Engineering, Information and Systems, University of Tsukuba, Tsukuba 305-8573, Japan

2. Structures Technology Division, Railway Technical Research Institute, Tokyo 185-8540, Japan

Abstract: The analysis used simple finite elements is performed to simulate the tensile behavior of corroded reinforcing bars extracted from three actual concrete structures. The cross-sectional area of the elements is set to have the actual distribution measured by 3D laser scanner system. The variable factor in the analysis is the length of the elements. The analysis results show that the length of the elements has a major influence on the deformation capacity after yielding. The calculated stress-strain curves, obtained using the elements with a length that is 2 times the bar diameter, are in good agreement with the tensile test results. The calculated stress-strain curves are modeled using a bi-linear model to facilitate the FEA (finite element analysis) of an overall concrete structure. From the analysis results, both the tensile and yield strengths decrease in proportion to the reduction of the minimum cross-sectional area of corroded bars. The ultimate strain has a remarkable decrement as the reduction of the minimum cross-sectional area. Formulas for determining these values are proposed as a function of the decrement ratio of the minimum cross-sectional area of a corroded bar.

Key words: Corroded bar, cross-sectional area distribution, minimum cross-sectional area, bi-linear model, ultimate strain.

1. Introduction

The corrosion of the reinforcing bars in RC (reinforced concrete) structures has become one of the most important issues affecting the structural performance of concrete structures that have been used for a long period. Especially, because the yield strength and elastic modulus of corroded reinforcing bars influence the structural performance of RC members, it is essential to be aware of their condition in order to evaluate the residual performance of RC structures. In addition, when the corrosion is particularly well advanced, the rupture of the corroded reinforcing bars could occur leading to the sudden loss of the load capacity or the collapse of RC structures. This indicates that an awareness of the residual elongation capacity of corroded reinforcing bars is also important for evaluating the performance of deteriorated RC.

There have been many studies on the mechanism of corrosion of reinforcing bars. However, only a small number of studies have been reported on the residual capacity of corroded bars in actual RC structures. Those bars were extracted from actual structures and had corroded due to chloride attack [1, 2] or concrete carbonation [3]. It has been pointed out that the accelerated corrosion differs from natural corrosion [4, 5]. When modeling actual RC structures, it is very important to be able to consider the mechanical properties of reinforcing bars that have corroded naturally. This paper discusses stress-strain modeling based on the cross-sectional area distributions observed in corroded reinforcing bars extracted from actual RC structures.

Several papers have reported the mechanical properties of corroded reinforcing bars. For example, Du et al. [6] investigated the yield strength and tensile

Corresponding author: Toshiyuki Kanakubo, Ph.D., associate professor, research fields: concrete materials, reinforcing materials and structural behavior of reinforced concrete members. E-mail: kanakubo@kz.tsukuba.ac.jp.

strength of corroded reinforcing bars and proposed a means of expressing their residual capacities as a function of the weight loss. Du et al. [6] also reported that the deterioration of elongation and ultimate strain of corroded reinforcing bars is much more significant than that of the yield and tensile strengths [7]. In contrast, Kim et al. [8] focused on the surface shape of corroded reinforcing bars and proposed stress-strain curves that are related to the maximum decrement of the cross-sectional area (decrement of the minimum cross-sectional area). It has been pointed out that the corrosion of reinforcing bars does not occur uniformly on the surface of the bar, e.g., Ref [9], and that the distribution of the degree of corrosion, which can be expressed as the cross-sectional area distribution, affects the mechanical properties of corroded reinforcing bars. Kashani et al. [10] investigated 3D corrosion patterns using an optical surface measurement technique and proposed a set of probabilistic distribution models for determining the geometrical properties of corroded bars.

The authors also focused on the cross-sectional area distributions of corroded reinforcing bars, investigating them using a 3D laser scanner system [11]. They reported that the maximum decrement of cross-sectional area is related to the average decrement of cross-sectional area, which is equivalent to the weight loss percentage. Du et al. [6] suggested that the non-uniform distribution of residual sections along the bar length affects the reduction of bar ductility and proposed a method of calculating the ultimate strain using the length coefficient of corrosion [7]. In other words, the distribution of different residual sections and the length of each influence the results of the calculation.

The goal of this study is to propose stress-strain curves for corroded reinforcing bars. The selected stress-strain model is a bi-linear model, as this is convenient for application to FEA (finite element analysis). Calculation, using a simple element model in which the cross-sectional area of each element is equal to that of the corroded bar along its length, is carried out, and the calculated results are compared with the tensile test results. To eliminate the influence of the element length on the calculation results, the element length is set to 1 mm, 0.5*d*, 1*d*, 2*d*, 4*d*, 8*d* and 16*d* (*d*: bar diameter). The cross-sectional area of each element is made equal to the measured value of the corroded reinforcing bars extracted from actual three RC structures and as measured with the 3D laser scanner system.

2. Investigated Reinforcing Bars and Tensile Test

2.1 Investigated Reinforcing Bars

Table 1 lists the investigated reinforcing bars extracted from three actual concrete structures. The total number of specimens is 12. All three structures were railroad-related structures. The Series A specimens were extracted from a slab that had been damaged by chloride attack. The structure was built in 1970 and used deformed bars of 10 mm in diameter (*D*10). The Series B specimens were extracted from a beam which had been deteriorated by carbonation. This structure was built in 1930 and so used round bars of 22 mm in diameter (ϕ22). The Series C specimens were extracted from a box culvert that had been damaged by chloride attack. The year of construction is not known. This used round bars of 19 mm in diameter (ϕ19).

Examples of the specimens are shown in Fig. 1. The

Table 1 Corroded reinforcing bars subjected to investigation.

Series	Type	Nominal diameter (mm)	Number of specimens	Extracted from	Corroded by
A (*D*10)	Deformed	10	6	Slab	Chloride
B (ϕ22)	Round	22	3	Beam	Carbonation
C (ϕ19)	Round	19	3	Wall	Chloride

photos were taken after rust had been removed. This was done by soaking the specimens in a citric acid solution. The Series A specimen, which had been damaged by chloride attack, exhibits a scooped-out surface in one area, while the other parts are not damaged. The Series B specimen, which had been corroded by carbonation, appears to have been scraped along the length of one side of the bar. The Series C specimen has both a scooped-out part and a rough surface along its entire length.

2.2 Cross-sectional Area Distribution of the Specimens

Cross-sectional area of the specimens was measured using a 3D laser scanner system [11]. The specimen was stood on a turntable, and the coordinates of the laser spot on the surface of the bar were measured. A set of coordinates for each section was obtained by rotating the turntable through 360° so that the cross-sectional area could be calculated. After measuring one section, the laser-spot was moved in the bar axis direction, and then the same measurement was performed for the next section. In this way, the distribution of the cross-sectional area could be obtained. We set the scanning pitch for the bar axis to 1 mm.

Fig. 2 shows examples of the cross-sectional area distribution of the specimens. The scanned length corresponds to a target length of 16*d* for the tensile test, explained in the next section. The dotted lines indicate the nominal cross-sectional area. The Series A specimen, which had been damaged by chloride attack, shows a remarkable decrement of cross-sectional area at one point, while the remainder of the specimen is basically unaffected, having the nominal cross-sectional area with fine "waves". These waves are a result of the ribs on the surface of the deformed bar. The Series B specimen, which had been corroded by carbonation, exhibits a similar cross-sectional area along the specimen length. The average and standard deviation of the cross-sectional

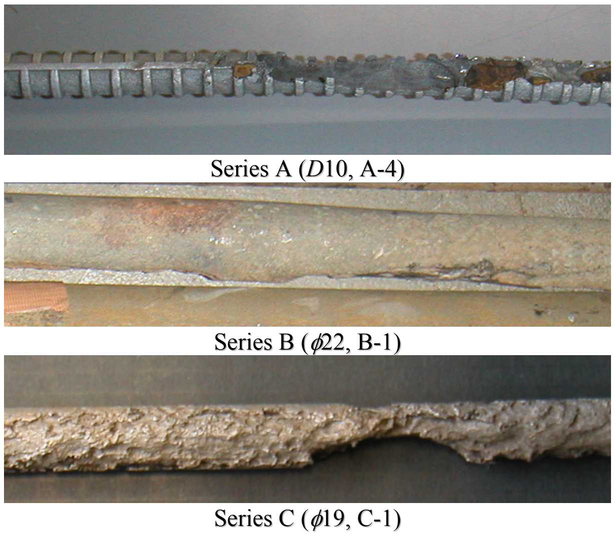

Fig. 1 Examples of corroded bars.

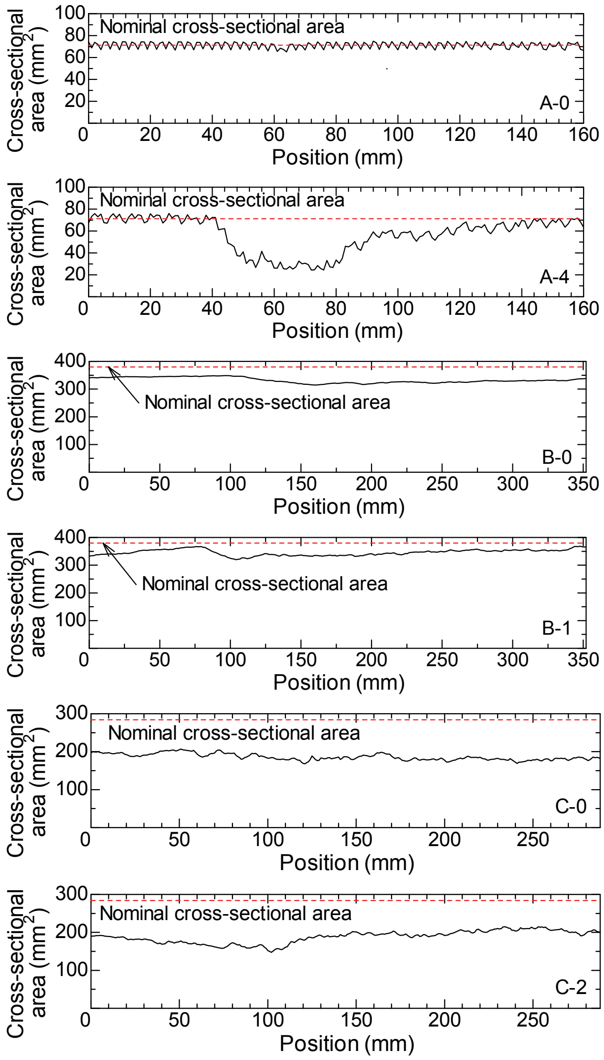

Fig. 2 Examples of cross-sectional area distribution of corroded bars.

area of B-1 specimen are 358.4 mm^2 and 9.3 mm^2, respectively. The Series C specimen exhibits a small amount of scattering and a notable decrement at a certain position. The average and standard deviation of the cross-sectional area of C-2 specimen is 187.9 mm^2 and 16.3 mm^2, respectively.

2.3 Tensile Test of Corroded Specimens

All 12 specimens were subjected to tensile tests with the local strains being measured with strain gauges and the elongation by LVDTs (linear variable displacement transducers). The target length used to measure the elongation was set to 16*d*. The tensile test setup is shown in Fig. 3. Target devices for LVDTs were attached to the specimens, and two LVDTs were set to measure the displacements of the target devices. The elongation was obtained as the sum of the two measured displacements. Two strain gauges were attached to the specimen, as shown in Fig. 4, with one gauge being at the position of the minimum cross-sectional area (Gauge C) and the other being at the maximum (Gauge N).

The tensile test results are summarized in Table 2. For this study, there is no non-corroded reinforcing bar to compare with the corroded ones because the specimens were extracted from actual structures that had been constructed at least several decades ago. However, to evaluate the influence of corrosion, it is

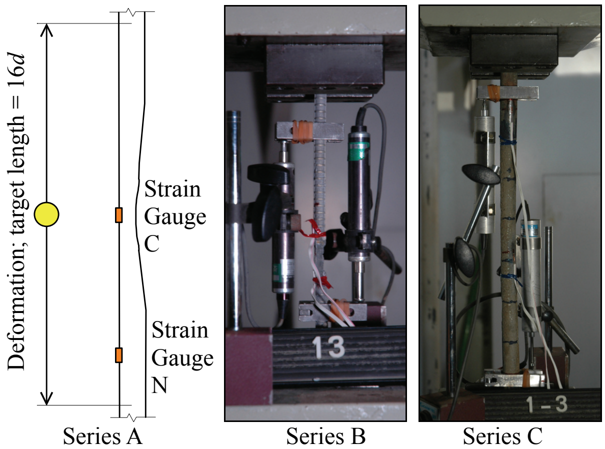

Fig. 3 Tensile test setup.

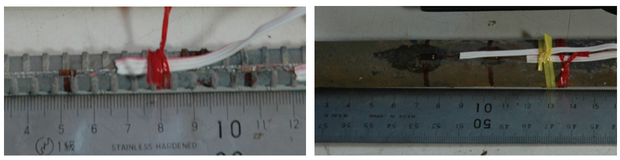

(a) (b)

Fig. 4 Strain gauge setup: (a) Series A; (b) Series B.

Table 2 Tensile test results.

Specimen		Minimum cross-sectional area (mm^2)	Tensile strength[a] (MPa)	Yield strength[a] (MPa)			Elastic modulus[a] (GPa)		
				From LVDT	From Gauge C	From Gauge N	From LVDT	From Gauge C	From Gauge N
A	A-0[b]	65.1	556	368	362	368	161	153	173
	A-1	62.9	409	373	-[e]	373	203	-[e]	199
	A-2	49.1	344	266[d]	-[e]	-[e]	118	-[e]	149
	A-3	48.4	371	295[d]	-[e]	-[e]	79.2	-[e]	174
	A-4	24.4	134	108[d]	-[e]	-[e]	88.4	-[e]	72.5
	A-5	27.9	183	-[e]	-[e]	-[e]	92.2	-[e]	-[e]
B	B-0[b]	314.7	461	324	328	328	199	196	194
	B-1	320.0	410	288	301	288	167	179	172
	B-2	320.9	410	319	310	319	169	-[e]	201
C	C-0[b]	167.9	359	257	265	266	197	156	178
	C-1[c]	62.2	135	83	-[e]	-[e]	22.1	-[e]	-[e]
	C-2	147.5	364	249[d]	240	288	127	191	189

[a]: Stress is calculated as tensile load divided by average cross-sectional area of non-corroded bar. Elastic modulus is obtained using those stresses;

[b]: These specimens are regarded as being non-corroded bars;

[c]: Target length was 3.5*d* (excluded from later discussions);

[d]: 0.2% offset strength;

[e]: Impossible to calculate.

essential to know the cross-sectional area and stress-strain curves for the corresponding non-corroded bars. Therefore, those specimens that exhibit the maximum tensile strength among the series of specimens, or which exhibit a clear yielding shelf in their stress-strain curves, are regarded as having similar properties to non-corroded bars. These specimens are designated A-0, B-0 and C-0 for the respective series specimens.

The stress-strain (Gauge N) curves of the A-0, B-0, and C-0 specimens are shown in Fig. 5. The stress is obtained from the measured tensile load divided by the average cross-sectional area of each specimen. The stress-strain curves of other specimens will be explained in Section 3. The tensile strength, yield strength and elastic modulus, listed in Table 2, are calculated using the average cross-sectional area of these specimens.

As shown in Table 2, the decrement of tensile strength generally corresponds to the minimum cross-sectional area. The yield strength determined from the stress-strain curves obtained from the LVDTs shows a similar tendency to the tensile strength. The yield strength and elastic modulus could not be obtained from the strain measured by the strain gauges for half of the specimens, because of the measurement of the small strain or compressive strain resulting from the eccentric loading due to the partial reduction in the cross-section by corrosion. The stress-strain curves measured by the LVDTs are discussed in the next section.

3. Tensile Behavior Analysis Using Cross-sectional Area Distribution

3.1 Analysis Method

Analyses using the cross-sectional area distribution of the specimens are conducted to enable the discussion of the tensile properties of the corroded reinforcing bars. The analysis model is shown in Fig. 6. The reinforcing bars are divided into simple finite elements for which the length and cross-sectional area are defined as L_i and A_i, respectively. The strain and elongation of each element is obtained by using the stress-strain curves for non-corroded bars, as shown in Fig. 5, at an arbitrary tensile load P. The total elongation ΔL is obtained by the sum of the elongations of each element. The average strain can be obtained as ΔL divided by the target length L. The stress-strain curves for the non-corroded bars are modified to be a monotonous increasing function, and linear interpolation data are applied to the calculation. The analysis is to be complete when the stress at the element with the minimum cross-sectional area reaches the tensile strength. The average strain at this calculation step is defined as ultimate strain.

3.2 Length of Elements

One of the research objectives of this study is to investigate the influence of the element length L_i on

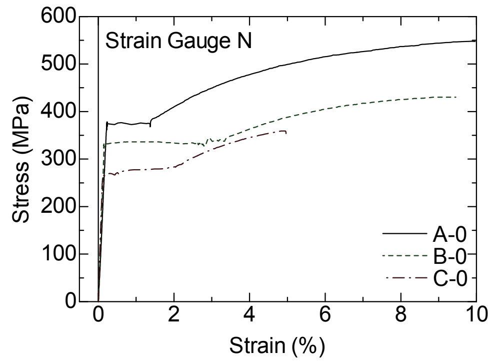

Fig. 5 Stress-strain curve of non-corroded bar.

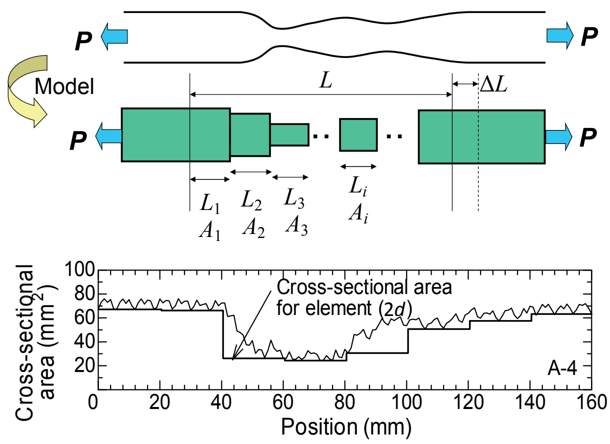

Fig. 6 Analysis model and exemplary distribution of A_i.

the calculation of the tensile characteristics. The cross-sectional area distributions of the specimens were measured at 1 mm intervals. The element length L_i is set to 1 mm, 0.5d, 1d, 2d, 4d, 8d and 16d. The minimum cross-sectional area in each element length L_i is adopted as A_i, as shown in Fig. 6. The target length is set to 16d, which is the same as that for the tensile test, so that the results of the analysis can be compared with the tensile test results. Therefore, the number of elements is 16 times d, 32, 16, 8, 4, 2 and 1 for the analysis of the element lengths of 1 mm, 0.5d, 1d, 2d, 4d, 8d and 16d, respectively.

3.3 Analysis Results

The calculated stress-strain curves for each corroded bar are shown in Figs. 7-9 (Series A, Series B and Series C), together with the tensile test results. The stress is obtained as the tensile load divided by the average cross-sectional area of the non-corroded bars (A-0, B-0 and C-0). Strain in the tensile test is obtained as the elongation measured by the LVDTs divided by the target length of 16d. The C-1 specimen is not included because of the short target length of the tensile test (3.5d). All of the diagrams show two graphs for each of the different element lengths used in the analysis.

In the Series A specimens (Fig. 7), it is recognized that the deformation capacity is remarkably affected by the difference of the element length. As expected, the ultimate strain becomes smaller for shorter element lengths, such as 1 mm. On the other hand, when the element length is long at 4d or more, larger ultimate

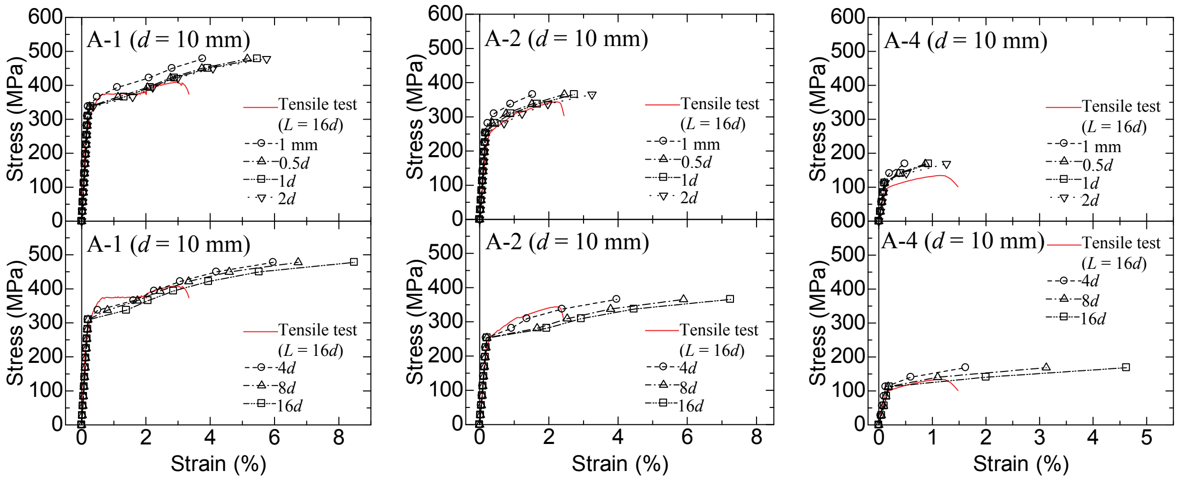

Fig. 7 Analysis results comparing with tensile test results (A-1, A-2 and A-4)

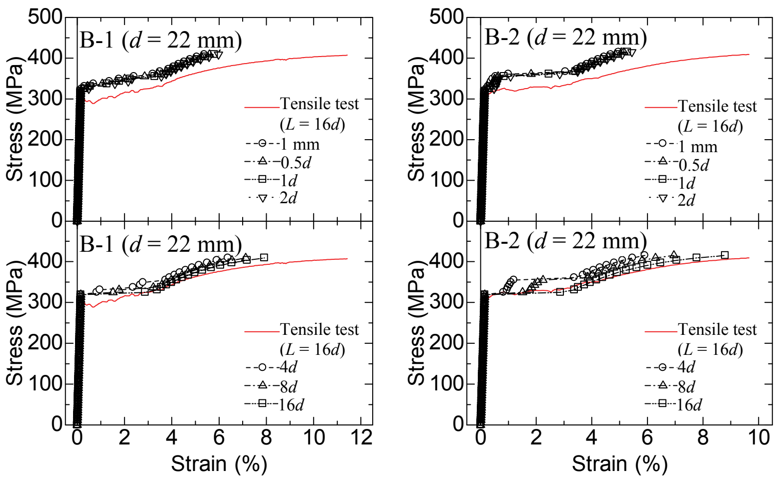

Fig. 8 Analysis results (B-1 and B-2).

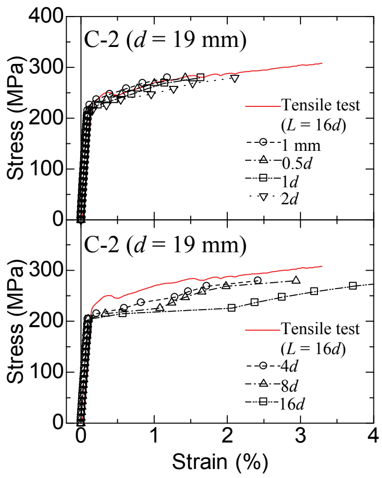

Fig. 9 Analysis results (C-2).

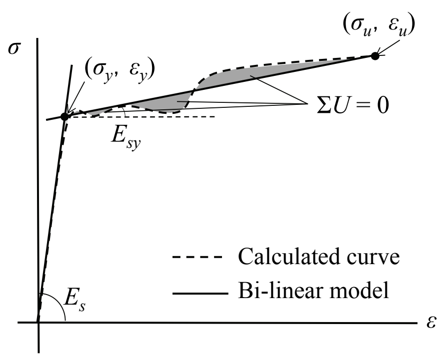

Fig. 10 Modeling method.

strain and less stiffness after yielding can be seen. It is considered that the ribs of deformed bars do not contribute greatly to the bar stiffness. For the Series B specimens (Fig. 8), the differences in the curves are not so clear as for the Series A specimens. Similar curves are obtained for the element lengths of 4d or less. For the Series C specimens (Fig. 9), a similar tendency to Series A specimens can be seen.

Therefore, it is considered that there is an optimum element length in the analysis to simulate the stress-strain curves for corroded reinforcing bars. For the corroded bars investigated in this study, the appropriate length proves to be around 2d.

4. Bi-linear Model of Stress-Strain Curve

4.1 Modeling Method

The calculated stress-strain curves determined in the previous section are modeled using a bi-linear model. The modeling is conducted for the curves calculated using the element length of 2d. The curves by 2d-element are generally considered to be suitable for expressing the tensile test results.

It is considered that the target length also influences the stress-strain curves, because the average strain is obtained as dividing by the target length. As described in the Introduction section, a bi-linear model of stress-strain curve is considered to be useful for application to FEA. The reinforcing bar elements are usually modeled as beam or truss models with lengths of several-hundred millimeters in the analysis of RC members or structures. Therefore, modeling is conducted for the target lengths of both 16d and 8d.

Fig. 10 shows the modeling method. The calculated stress-strain curve is indicated by the dotted line. The bi-linear model is characterized by elastic modulus E_s, yield strength σ_y and yield strain ε_y, tensile strength σ_u and ultimate strain ε_u and secondary modulus E_{sy}. The elastic modulus, tensile strength and ultimate strain can be obtained directly by the analysis described in Section 3. The elastic modulus is calculated from the average cross-sectional area, implying that the elastic modulus is equivalent to the average stiffness of each element. The tensile strength and ultimate strain are defined as being the stress and strain at the point where the stress in the element with the minimum cross-sectional area reaches the maximum. The secondary modulus is decided to be that at which the summation of the strain energy (ΣU) enclosed by the dotted curve and the bi-linear model becomes zero after yielding. Then, the yield strength and strain can be obtained from the point, at which the first and second lines intersect.

4.2 Model for Target Length of 16d

A list of the minimum and average cross-sectional area of the modeled bars is shown in Table 3. The decrement ratios of the minimum and average cross-sectional area are defined as dividing by the average cross-sectional area of the non-corroded bars

Table 3 Sectional area of modeled bars (16*d*).

Specimen		Minimum cross-sectional area (mm²)	Decrement ratio[c] r_{min} (%)
A	A-0[a]	(71.1)[b]	-
	A-1	62.9	11.53
	A-2	49.1	30.94
	A-3	48.4	31.93
	A-4	24.4	65.68
	A-5	27.9	60.76
B	B-0[a]	(332.4)[b]	-
	B-1	320.0	3.73
	B-2	320.9	3.46
C	C-0[a]	(186.1)[b]	-
	C-2	147.5	20.74

[a]: regarded as being non-corroded bars;
[b]: average cross-sectional area;
[c]: ratio to average cross-sectional area of non-corroded bars.

(A-0, B-0 and C-0).

The bi-linear models for the stress-strain curves are shown in Fig. 11. The figures also include the calculated stress-strain curves obtained with the 2*d*-element, the tensile test results and stress-strain models proposed by Kim et al. [8]. As expected, elastic modulus, tensile strength and ultimate strain of the bi-linear model are in precise agreement with the calculated curves.

Table 4 lists the characteristic values of the model for the target length of 16*d*. The table also includes the ratio of the yield strength of the model to the tensile test results listed in Table 2. The yield strength of the bi-linear model is higher than that of the calculated curves for some specimens, but lower for others. The yield and tensile strengths of the bi-linear model show an almost linear relationship with the decrement ratio of the minimum cross-sectional area. It is clear that the tensile strength can be characterized by the minimum cross-sectional area but not by either the average cross-sectional area or weight loss. The secondary modulus exhibits a tendency to increase as the decrement ratio of the minimum cross-sectional area becomes larger. The ultimate strain is very sensitive to the decrement ratio of the minimum cross-sectional area. The elongation of the elements is not particularly large at the ultimate, where only the element which has the minimum area attains to ultimate.

4.3 Model for Target Length of 8d

The same modeling, as that described in Section 4.2, is conducted for the target length of 8*d*. The cross-sectional area distributions of the half-length from the central positions of the corroded reinforcing bars investigated as part of this study are focused and designated *L* and *R*. The objective of the modeling described in this section is to discuss the influence of the target length on the characteristic values of the

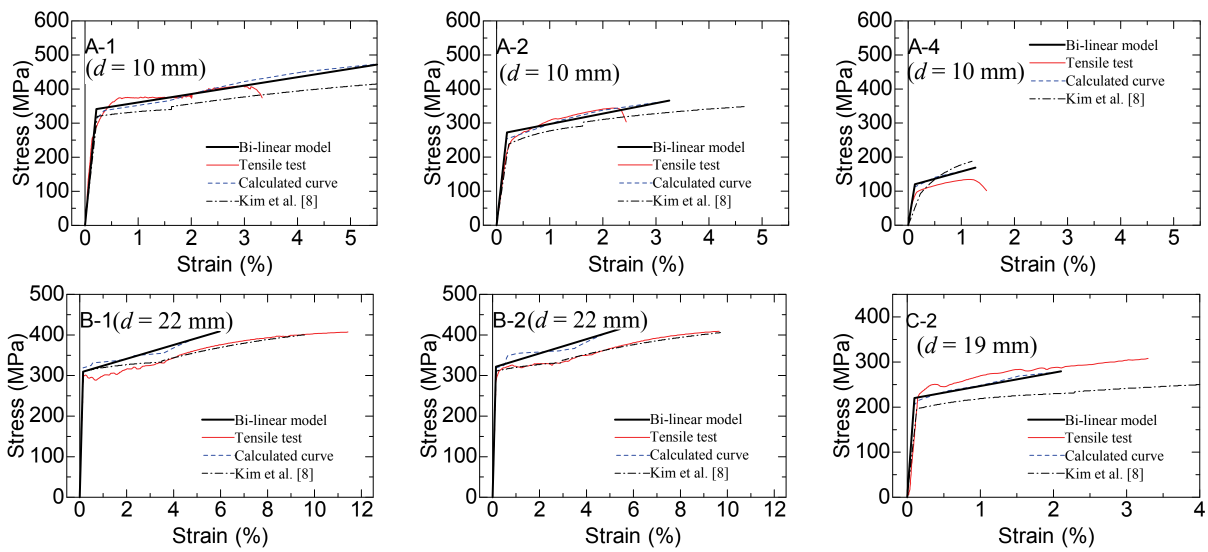

Fig. 11 Bi-linear model for target length of 16*d*.

Table 4 Characteristic values of bi-linear model for target length of 16*d*.

Specimen		Yield strength σ_y (MPa)	Yield strength Model/test	Yield strain ε_y (%)	Elastic modulus E_s (GPa)	Tensile strength σ_u (MPa)	Ultimate strain ε_u (%)	Secondary modulus E_{sy} (GPa)
A	A-0[a]	411	1.12	0.237	173	548	9.97	0.141
	A-1	341	0.91	0.214	160	478	5.75	0.247
	A-2	272	1.02	0.196	139	366	3.25	0.306
	A-3	280	0.95	0.203	138	366	3.32	0.275
	A-4	120	1.11	0.126	96	169	1.27	0.426
	A-5	152	-	0.139	109	197	1.22	0.416
B	B-0[a]	325	1.00	0.167	194	430	9.45	0.114
	B-1	310	1.08	0.142	218	409	5.97	0.171
	B-2	322	1.01	0.142	226	415	5.43	0.176
C	C-0[a]	257	1.00	0.144	178	359	4.96	0.212
	C-2	220	0.88	0.098	224	280	2.10	0.297

[a]: regarded as being non-corroded bars.

Table 5 Sectional area of modeled bars (8*d*).

Specimen		Minimum cross-sectional area (mm^2)	Decrement ratio[c] r_{min} (%)
A	A-0[a]	(71.1)[b]	-
	A-1 L/R	68.1 / 62.9	4.22/11.53
	A-2 L/R	49.1 / 53.0	30.94/25.46
	A-3 L/R	48.4 / 53.4	31.93/24.89
	A-4 L/R	24.4 / 30.6	65.68/56.96
	A-5 L/R	64.1 / 27.9	9.85/60.76
B	B-0[a]	(332.4)[b]	-
	B-1 L/R	320.0 / 332.0	3.73/0.12
	B-2 L/R	320.9 / 354.2	3.46/−6.56
C	C-0[a]	(186.1)[b]	-
	C-2 L/R	147.5/196.3	20.74/−0.11

[a]: regarded as being non-corroded bars;
[b]: average cross-sectional area;
[c]: ratio to average cross-sectional area of non-corroded bars.

bi-linear model. A list of the minimum and average cross-sectional area for the 8*d* target length is given in Table 5. The decrement ratios of the minimum and average cross-sectional area are defined as being obtained by dividing by the average cross-sectional area of the non-corroded bars (A-0, B-0 and C-0). The decrement ratios are negative for some specimens meaning that the minimum or average cross-sectional area for the length in question is larger than the average cross-sectional area of Specimens B-0 and C-0. Some of the Series A and C-2 Specimens exhibit large differences between *L* and *R* because of the partial corrosion.

Examples of the bi-linear models of the stress-strain curves for the target length of 8*d* are shown in Fig. 12. The figures also include the stress-strain curves calculated using the 2*d*-element and the stress-strain models proposed by Kim et al. [8]. The tensile test was carried out for those specimens with the 16*d* target length, so there are no tensile test results for the 8*d* target length. As expected, the calculated curves and the model differ greatly between *L* and *R* due to the differences in the cross-sectional area distribution. In general, the ultimate strain becomes larger than that for the 16*d* target length. Table 6 lists the characteristic values of the model for the 8*d* target length.

4.4 Evaluation of Characteristic Values

The evaluation of the characteristic values of the bi-linear model is described in this section. Considering the results given in Sections 4.2 and 4.3, the bi-linear model is considered to be affected by the minimum cross-sectional area rather than the average cross-sectional area, which is equivalent to the weight loss percentage. The stress-strain curves proposed by Kim et al. [8] are also described by the minimum cross-sectional area. For example, it is easily understood that the tensile strength and elastic limitation can be determined from the minimum cross-sectional area.

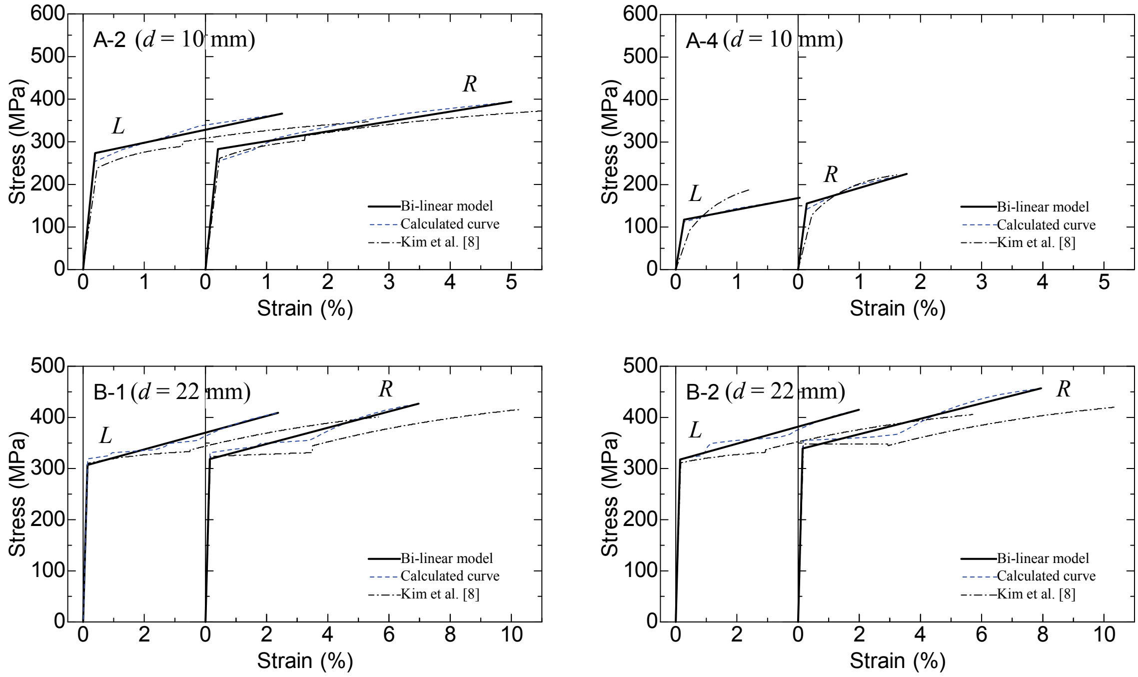

Fig. 12 Bi-linear model for target length of 8*d*.

Table 6 Characteristic values of bi-linear model for target length of 8*d*.

Specimen		Yield strength σ_y (MPa)	Yield strain ε_y (%)	Elastic modulus E_s (GPa)	Tensile strength σ_u (MPa)	Ultimate strain ε_u (%)	Secondary modulus E_{sy} (GPa)
A	A-0[a]	411	0.237	173	548	9.97	0.141
	A-1 L/R	361/341	0.220/0.220	164/155	506/478	6.67/6.78	0.225/0.208
	A-2 L/R	274/283	0.196/0.205	140/138	366/394	3.25/5.00	0.302/0.232
	A-3 L/R	280/294	0.205/0.213	137/138	366/394	3.67/4.33	0.249/0.244
	A-4 L/R	117/155	0.137/0.142	86/109	169/225	2.03/1.78	0.273/0.426
	A-5 L/R	351/152	0.241/0.175	146/87	478/197	7.05/2.31	0.186/0.212
B	B-0[a]	325	0.167	194	430	9.45	0.114
	B-1 L/R	307/319	0.143/0.144	215/221	409/439	6.38/6.96	0.164/0.159
	B-2 L/R	318/339	0.143/0.147	222/231	415/457	5.99/7.94	0.166/0.151
C	C-0[a]	257	0.144	178	359	4.96	0.212
	C-2 L/R	212/256	0.105/0.106	202/241	279/355	3.30/4.08	0.208/0.250

[a]: regarded as being non-corroded bars.

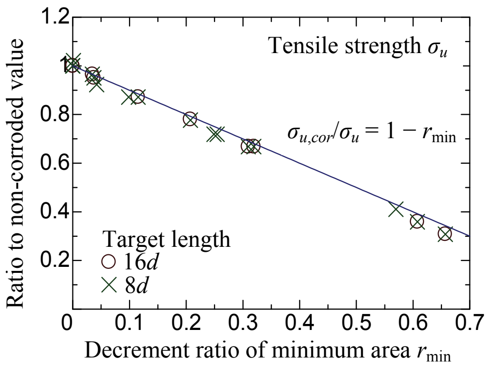

Fig. 13 Tensile strength—decrement ratio relationship.

The relationship between the ratio of the tensile strength of the corroded bar to that of non-corroded bar in the bi-linear model and the decrement ratio of the minimum cross-sectional area is shown in Fig. 13. The data with negative decrement ratios are omitted. As expected, the plots form an almost straight line from the *y*-intercept of 1. The slight differences between the plots and the line are due to the analysis method explained in Section 3.1, as the analysis is carried out discretely for the tensile load. The form of

Eq. (1) is usually used to express the reduction in the characteristic values of the corroded reinforcing bars. In the case of Fig. 13, the coefficient k for the decrement ratio is equal to 1:

$$\frac{v_{cor}}{v} = 1 - k \cdot r_{min} \tag{1}$$

where:

v_{cor}: characteristic value for corroded reinforcing bar;

v: characteristic value for non-corroded reinforcing bar;

k: coefficient for decrement ratio;

r_{min}: decrement ratio of minimum cross-sectional area.

Similarly, the relationship between the ratio of the characteristic values (yield strength, yield strain, secondary modulus and ultimate strain) of the corroded bar to those of non-corroded bar, as well as the decrement ratio of the minimum cross-sectional area, is shown in Figs. 14-17. The data with negative values for the decrement ratio are omitted.

The yield strength of the bi-linear model in this study shows both higher and lower value than that indicated by the calculated curves. From Fig. 14, the yield strength of the model is in reasonably close agreement with the line shown in the figure, for which the coefficient of the decrement ratio is equal to 1. The value of the yield strain is larger than that indicated by the line for the coefficient for the decrement ratio of 1. Regression analysis by the least square method gives the formula shown in Fig. 15. It can be deduced that the yield strain, which is given as the yield strength divided by the elastic modulus, is affected by both the minimum and the average cross-sectional area of the corroded reinforcing bar. The result of the evaluation of the corroded bars addressed in this study shows the coefficient of the decrement ratio of 0.64.

The secondary modulus becomes larger together with the decrement ratio (Fig. 16). The increment tendencies for the target lengths of 16d and 8d are different, with the two lines in the figure being drawn by regression analysis. The number of elements with a

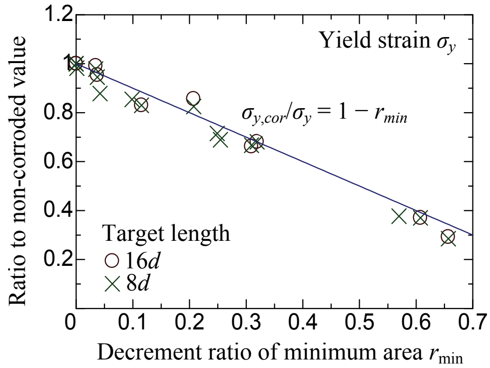

Fig. 14 Yield strength—decrement ratio relationship.

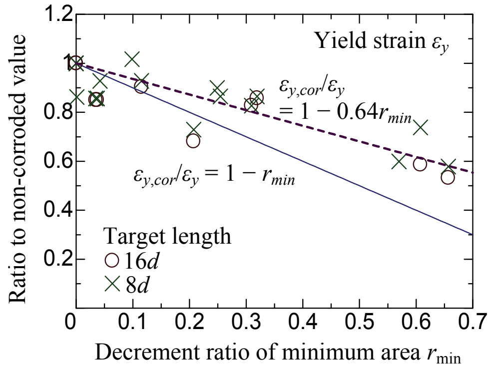

Fig. 15 Yield strain—decrement ratio relationship.

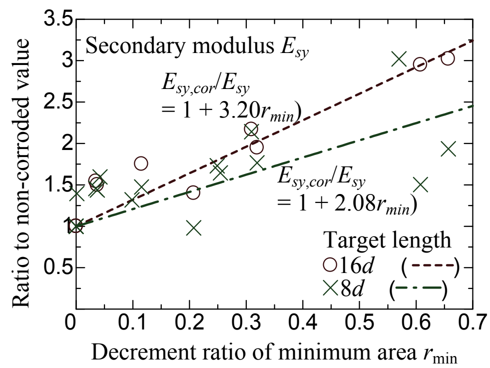

Fig. 16 Secondary modulus—decrement ratio relationship.

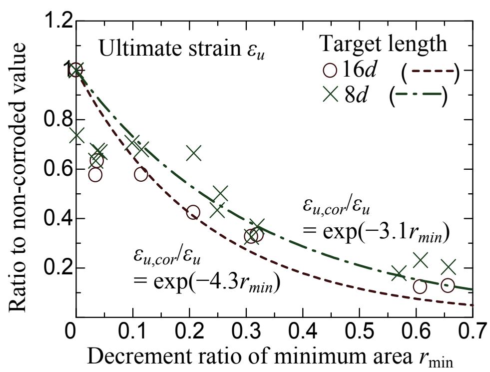

Fig. 17 Ultimate stain—decrement ratio relationship.

relatively smaller cross-sectional area decreases as the target length becomes larger. This results in an increase in the stiffness after yielding.

The decrement of ultimate strain is remarkable when compared with other characteristics, such as the yield strength or tensile strength (Fig. 17). The decrement tendencies for the 16*d* and 8*d* target lengths are also different, because the number of elements in which the strain is not so large increase when one element with the minimum cross-sectional area reaches ultimate in case of large target length. The two curves are obtained by regression analysis, as shown in Fig. 17.

From the results shown in Figs. 15-17, it is possible to derive the following formulas. The characteristic values of the bi-linear model for the corroded reinforcing bar for which the minimum cross-sectional area is known can be estimated by using these formulas:

$$\frac{\varepsilon_{y,cor}}{\varepsilon_y} = 1 - 0.64 \cdot r_{min} \tag{2}$$

$$\begin{cases} \dfrac{E_{sy,cor}}{E_{sy}} = 1 + 3.20 \cdot r_{min} \quad (16d \text{ target length}) \\ \dfrac{E_{sy,cor}}{E_{sy}} = 1 + 2.08 \cdot r_{min} \quad (8d \text{ target length}) \end{cases} \tag{3}$$

$$\begin{cases} \dfrac{\varepsilon_{u,cor}}{\varepsilon_u} = \exp(-4.3 \cdot r_{min}) \quad (16d \text{ target length}) \\ \dfrac{\varepsilon_{u,cor}}{\varepsilon_u} = \exp(-3.1 \cdot r_{min}) \quad (8d \text{ target length}) \end{cases} \tag{4}$$

where:

r_{min}: decrement ratio of minimum cross-sectional area;

ε_y: yield strain;

E_{sy}: secondary modulus;

ε_u: ultimate strain; the subscript *cor* indicates the corroded reinforcing bar.

5. Conclusions

An analysis is conducted using the cross-sectional area distributions of corroded reinforcing bars that had been extracted from three actual concrete structures. The objective of the analysis is to investigate the influence of the element length on the tensile characteristics of the corroded reinforcing bars. There is an optimum length for the element in the analysis to simulate the stress-strain curves of the corroded reinforcing bars. It is considered that the appropriate length for the corroded bars investigated in this study is around 2*d*.

Bi-linear modeling for the target lengths of both 16*d* and 8*d* is performed for the calculated stress-strain curves. The modeling results show that the tensile and yield strengths decrease in proportion to the reduction in the minimum cross-sectional area of the corroded bars. The decrement of the yield strain is gradual rather than tensile and yield strengths. The secondary modulus of the bi-linear model increases as the minimum cross-sectional area decreases. The ultimate strain at the tensile strength shows a remarkable decrement with the reduction of the minimum cross-sectional area. Formulas to evaluate these characteristic values are proposed as functions of the decrement ratio of the minimum cross-sectional area of the corroded bars.

The results of the modeling and the proposed formulas only indirectly express the shape of the cross-sectional area distributions of the corroded reinforcing bars extracted from three actual concrete structures. It should be noted that different tendencies in the cross-sectional area distributions gives different results. Further investigation is necessary to better understand this.

Acknowledgments

The authors express their gratitude and sincere appreciation to the members of the Japan Concrete Institute Technical Committee, Structural and Durability Evaluation for Corroded Concrete Structures (JCI-TC112A). The authors also acknowledge Mr. Satoshi Ogawa for performing the analysis work.

References

[1] Morinaga, S. 1996. “Remaining Life of Reinforced

Concrete Structures after Corrosion Cracking." *Durability of Building Materials and Components* 1: 127-37.

[2] Palssom R., and Mirza, M. S. 2002. "Mechanical Response of Corroded Steel Reinforcement of Abandoned Concrete Bridge." *ACI Structural Journal* 99 (2): 157-62.

[3] Zhang, P. S., Lu, M., and Li, X. Y. 1995. "The Mechanical Behaviour of Corroded Bar." *Journal of Industrial Buildings* 25 (257): 41-4.

[4] François, R., Khan, I., and Dang, V. H. 2013. "Impact of Corrosion on Mechanical Properties of Steel Embedded in 27-Year-Old Corroded Reinforced Concrete Beams." *RILEM Materials and Structures* 46: 899-910.

[5] Yuan, Y., Ji, Y., and Shah, S. P. 2007. "Comparison of Two Accelerated Corrosion Techniques for Concrete Structures." *ACI Structural Journal* 104 (3): 344-7.

[6] Du, Y. G., Clark, L. A., and Chan, A. H. C. 2005. "Residual Capacity of Corroded Reinforcing Bars." *Magazine of Concrete Research* 57 (3): 135-47.

[7] Du, Y. G., Clark, L. A., and Chan, A. H. C. 2005. "Effect of Corrosion on Ductility of Reinforcing Bars." *Magazine of Concrete Research* 57 (7): 407-19.

[8] Kim, H., Tae, S., Lee, H., Lee, S., and Noguchi, T. 2009. "Evaluation of Mechanical Performance of Corroded Reinforcement Considering the Surface Shape." *ISIJ International* 49 (9): 1392-400.

[9] Kranc, S. C., and Sagues, A. A. 2001. "Detailed Modeling of Corrosion Macrocells on Steel Reinforcing in Concrete." *Corrosion Science* 43 (7): 1355-72.

[10] Kashani, M. M., Crewe, A. J., and Alexander, N. A. 2013. "Use of 3D Optical Measurement for Stochastic Corrosion Pattern Analysis of Reinforcing Bars Subjected to Accelerated Corrosion." *Corrosion Science* 73: 208-21.

[11] Oyado, M., Kanakubo, T., Yamamoto, Y., and Sato, T. 2011. "Bending Performance of Reinforced Concrete Member Deteriorated by Corrosion." *Structure and Infrastructure Engineering* 7 (1-2): 121-30.